Protection in a model of liver injury is parallel to energy mobilization capacity under distinct nutritional status

Bérengère Papegay, Vincent Nuyens, Adelin Albert, Mustapha Cherkaoui-Malki, Oberdan Leo, Véronique Kruys, Jean G. Boogaerts, Joseph Vamecq

Protection in a model of liver injury parallels to energy mobilization capacity under distinct nutritional status

Bérengère Papegay, MD[a], Vincent Nuyens, BSc[a], Adelin Albert, PhD[b], Mustapha Cherkaoui-Malki, PhD[c], Oberdan Leo, PhD[d], Véronique Kruys, PhD[d], Jean G. Boogaerts, MD, PhD[a], Joseph Vamecq, MD, PhD[e,*]

[a] Divisions of Experimental Medicine (ULB Unit 222), University Hospital Center, Charleroi, Belgium

[b] Department of Biostatistics, University Hospital of Liège, Liège, Belgium,

[c] Université de Bourgogne-Franche Comté, Laboratoire BioPeroxIL (Biochimie du Peroxysome, Inflammation et Métabolisme Lipidique) EA 7270, Dijon, France

[d] Immunobiology and Molecular Biology of the Gene, Department of Molecular Biology, Free University of Brussels (ULB), Gosselies, Belgium

[e] Inserm, Biochemistry and Molecular Biology Laboratory , HMNO, CBP, CHRU Lille & EA 7364 – RADEME, North France University Lille, France.

*** Correspondance** : Joseph Vamecq, MD, PhD, Inserm, HMNO-CBP, Secteur Métabolisme, CHRU Lille, 2, Bd Jules Leclercq, 59037 Lille, France. Phone:+33320445694; FAX:+33320445693; Email : joseph.vamecq@inserm.fr

Running head

Nutritional status and liver energy mobilization

Financial disclosure: none declared.

*** Corresponding author:** Tel.: +33 320445694; fax +33 320445693.

E-mail address: joseph.vamecq@inserm.fr (J. Vamecq)

Abstract

Objective: Dietary and energetic restrictions are endowed with protection against experimental injuries. However, a drop of cell energetic status under a critical threshold may prevent protection as previously observed for livers isolated from rat donors undergoing 18h-fasting *vs* feeding. In this latter model, links between nutritional status, energy availability and protection are further explored through lengthening of rat fasting to 24h and withdrawal of energy sources from perfusions.
Methods: Energy-free perfused *ex vivo* livers from fed, 18h- and 24h-fasted rats were studied during 135min for cytolysis (potassium, ALT, AST, LDH releases in perfusates), cell deaths (activated caspase-3 [apoptosis], LC3II/actin and p62/actin ratios [autophagy]), glycogen stores, glucose and lactate productions.
Results: Cytolysis was significantly increased by 18h- and 24h-fasting *vs* feeding but unexpectedly lowered by 24h- *vs* 18h-fasting. Apoptotic marker caspase 3 significantly increased under fed and 18h-fasting but not 24h-fasting conditions. Autophagic marker LC3II/actin significantly increased during perfusion in 24h-fasting group but neither fed nor 18h-fasting groups. Autophagic induction was also supported by a drop in p62/actin ratio. Under perfusion with 3-methyladenine, a standard autophagy inhibitor, protection and enhanced autophagy provided by 24h- *vs* 18h-fasting were lost without affecting apoptosis.
Conclusions: Liver protections are obviously influenced by nutritional status in a way here paralleling to hepatic energy mobilization capacities (glycogen plus autophagy) with in decreased order of protections: fed>24h-fasted>18h-fasted>24h-fasted+3MA livers. By showing that autophagy induction limits starvation-induced cytolysis, the present work supports the emerging view that autophagy inducers might improve health benefits of diet restriction.

Introduction

The protective properties of dietary and energetic restrictions in health, ageing and disease models assessed through experimental injuries have been previously considered along with the counterbalanced view that a drop of cell energy availability under a critical threshold may prevent protection [1]. This latter aspect was inferred from studies on livers isolated from rat donors undergoing 18h-fasting *vs* feeding, and showing an exacerbation by 18h-fasting of *ex vivo* liver cytolysis [1]. In this respect, necrosis, apoptosis and autophagy represent cell deaths which are accidental, programmed and programmed with optional survival, respectively [2,3]. Extrinsic and intrinsic apoptosis recruit plasma membrane (death-inducing signalling complex DISC) and soluble apoptosomes, respectively [4] to trigger auto-activation of initiating caspases which in turn activate executioner caspases for protein cleavage and changes observed during apoptosis [5]. Autophagy involves autophagosomes (encompassing intracytoplasmic components and organelles) which fuse with lysosomes for content degradation; it may lead to cell death or under nutrient deprivation [6] supply energy compatible with cell survival [7].

As mentioned above, exacerbation of cytolysis and drop under a critical energy threshold were previously documented in *ex vivo* perfused livers originating from 18h-fasted *vs* fed rats [1,8]. The primary goal of carrying out the present study was to work under energy deprived perfusion and to perform a lengthening of starvation period which precedes liver isolation. This latter was done to provide an additional exacerbation of fasting-driven susceptibility to liver cytolysis previously reported in our liver model [1]. The reason of this strategy was to amplify and hence better characterize key determinants responsible for the difference observed in cytolysis between fed and starved states. Unexpectedly, the exacerbation of cytolysis was reduced by increasing starvation period. This has led, secondarily, to consider mechanisms which might protect against fasting-driven cytolysis. In fact, assessing cell death pathways (apoptosis and autophagy) along with energetic stores in various nutritional states here leads to better understand the two issues in our liver model: differences in cytolyses between fed and starved states and mechanisms which might protect against fasting-driven exacerbation of cytolysis. Apoptosis is monitored by changes in activated caspase-3 (extrinsic and intrinsic apoptosis) [9]. Autophagy is assessed by increase in LC3II/actin ratio (and decrease in p62/actin ratio) [10-12], and is modulated by 3-methyladenine (3MA), a specific inhibitor of autophagy [13].

Materials and methods

Ethics

All animal studies were authorized by the Animal Care Use and Review Committee of the Belgian Free University of Brussels (CEBEA-IBMM-2014-39).

Animals

Female Wistar rats purchased from Charles River Laboratories (Saint Germain Nuelles, France) with a body weight of 200 g were acclimatized for at least five days to the room temperature of 24-26°C with a 12:12-h light-dark cycle. Standard laboratory chow and water were provided *ad libidum.* Animals were randomly allocated to fed (n=15) and fasting groups ($n \geq 10$ in each group), 18h (n=15) and 24h (n=10)-fasted groups keeping free access to tap water, with food withdrawn 18 and 24h before liver isolation, respectively. Challenge of 24h-fasted group by 3-methyladenine (3MA) (n=10) was done by compound inclusion in perfusion of removed livers, avoiding animal exposure to *in vivo* compound side effects.

Solutions and chemicals for liver perfusions

Albumin-free Hank's Balanced Salt Solution (HBSS) included 0.4 g/L KCl, 0.06 g/L KH_2PO_4, 0.35 g/L $NaHCO_3$, 0.048 g/L Na_2HPO_4, and 0.14 g/L $CaCl_2$. HEPES 2.38 g/L were added. All these chemicals were obtained from Sigma (Bornem, Belgium). The solution was saturated with 100% O_2 (0.5 L/min), pH adjusted to 7.35±0.05 using NaOH 1.0 M and supplemented with NaCl to achieve 300 mOsm. In part of experiments with livers from 24h-fasted rats, HBSS mixture contained 5 mM 3MA (Sigma-Aldrich, Bornem, Belgium). 24h-Fasting+3MA and 24h-fasting groups were perfused by HBSS mixtures supplemented and not with 5 mM 3MA, respectively.

Hepatectomy and ex vivo liver perfusion

Procedure for liver removal and perfusion was extensively described elsewhere [8,14]. Briefly, animals were anesthetized with pentobarbital sodium (NEMBUTAL®, Ceva, Libourne, France) intraperitoneally (50 mg/kg), the abdomen was opened and heparin (5000 IU/kg) administered *via* the inferior vena cava. The portal vein was cannulated with a 22-gauge catheter, secured in place and immediately perfused with the adequate solution. The liver was removed under continuous perfusion and transferred to the closed system *ex vivo* arrangement. The system (circuit volume of 125 mL) was maintained at 37°C. The perfusate, i.e., enriched HBSS solution supplemented or not with 5 mM 3MA, passed sequentially through a peristaltic pump (ISMATEC REGLO, Fisher Bioblock Scientific, Tournai, Belgium) at a flow rate of 5 mL/min to obtain a perfusion pressure around 12 cm H_2O through the portal vein.

General protocol for liver biopsies and perfusate sampling

Protocol included 135 min perfusion of livers with respective solutions. Perfusate samples were collected every 15 min and thin liver biopsies at 0 and 135 min with instantaneous immersion in either liquid nitrogen with storage at –80°C before determination of LC3II and p62 autophagy marker or in 10% formalin before postponed embedding in paraffin before immunohistochemistry of caspase-3 (apoptosis) and periodic acid Schiff staining (glycogen). For apoptosis, livers embedded in paraffin were cut by a microtome with deposition of slices on optic microscopic glasses. These latter were kept at room temperature for 24 hours before deparaffinisation and processing for caspase 3 immunostaining mentioned below in the experimental subsection titled "Apoptosis and Caspase-3".
For PAS staining, liver slice deparaffinisations and staining with periodic acid were performed by a Tissue Tek Prisma® apparatus (Sakura, Europe). PAS stained slices were processed for determination of glycogen contents in hepatocytes at two time-points, i.e. 0 and 135 min, using the Image J software (National Institutes of Health, Bethesda, MD, USA) [14]. Five fields per PAS stained slide were analyzed by a video-microscope (LEITZ DIALUX 20ES, Leitz, Wetzlar, Germany) equipped with a x40 objective and combined with a personal computer [8]. Generated pictures were captured onto the hard drive of the workstation computer. Thereafter, captured images were opened in Image J program (NIH, Bethesda, Maryland, USA) for evaluating indices of positivity on PAS slides. We selected the threshold of glycogen content of all cells (X value) and we referred it to the surface of all cells (Y value). From these area data, the glycogen index for the image was calculated, and expressed as a percentage (X/Y).

Perfusate markers and liver biopsy glycogen contents

Aspartate aminotransferase (AST, IU/L), alanine aminotransferase (ALT, IU/L), lactate dehydrogenase (LDH, IU/L), glucose (mg/dl), lactate (mmol/L), and potassium (mEq/L) were assayed in perfusate samples on a Architect plus CI4100 (Abbott Diagnostics, IL, USA). Glycogen contents were determined as mentioned above.

Apoptosis and caspase-3

Apoptosis was evaluated in a blinded fashion using light microscopy after *in situ* immunostaining. Deparaffinised liver sections were pre-treated: hot citrate buffer pH 6, inhibition of endoperoxydases

with methanol/H_2O_2 blocking cross-reaction (Immunologic, Duiven, The Netherlands) and inhibition of endo-biotin (Vector, Burlingame, CA, USA). Slides were incubated at 4°C overnight using a specific primary antibody for activated cleaved Caspase-3 (CASPASE-3 ASP 175, Cell Signalling Technology, Danvers, MA, USA) at a 1:100 dilution. Signal amplification was performed with incubation of the complex Ultrasens Streptavidin Peroxidase RTU (Immunologic, Duiven, The Netherlands). Revelation was done with diaminobenzidine (Biogenex, Fremont, CA, USA). Slides were counterstained with Toluidine Blue. Apoptosis activity was expressed as the percentage of apoptotic cells (reported on number of hepatocytes) in selected regions. Five fields of each stained slide were analysed. Apoptosis counting was performed with the image J software using a selection of cells immunolabelled for activated caspase-3, a determination of total and labelled cells by the image J cell counter and a subsequent calculation of labelled to total liver cell ratios.

Autophagy, LC3II and p62 to actin ratios

LC3II and actin were assayed by western blot. After defrosting from -80°C, liver biopsies were weighed and protein concentrations determined to load western blot gels with similar amounts of proteins. Biopsy was grinded in a micro-vial containing a protease inhibitor (mini EDTA free pellets, Roche, Basel, Switzerland), PBS and Lysing Matrix D Bulk on a Fast Prep Instrument (MP Biomedicals, Santa Ana, CA, USA). It was diluted in a Laemmli buffer (Tris 60 mM pH 6.8, 10% glycerol, 0.01% bromophenol blue, 5% β-mercaptoethanol, 2% SDS) to disrupt disulfide bonds and negatively charge proteins for size-based separation. One µl Benzonase (Novagen, EMD Millipore Corporation, Temecula, CA, USA) was added. Samples were heated to denature proteins, loaded in wells in 10% polyacrylamide/bisacrylamide gel (PAGEr ™ EX Gels, Lonza , Rockland, ME USA) in a ProSieve ™ Ex Running Buffer (Lonza , Rockland , ME, USA) and submitted to 100 volts for 10 minutes, and 150 volts until complete migration of the markers. Gel was transferred onto membrane using a transfer buffer (25mM Tris pH 7.6, 192 mM Glycine, 0.03% SDS, 20% methanol) under 100 Volts during 2h at 4°C, checking complete transfer of proteins with Red Ponceau. Membrane was incubated for 1 h in TBST + 5% milk at room temperature before incubation with a primary antibody LC3B (# 2775, rabbit 1: 1000, Cell Signalling Technology, Danvers, MA, USA) at 4° C overnight. For LC3II detection, a HRP-coupled secondary antibody (Promega, Madison, WI USA) was added 40 minutes at room temperature and stirred for chemiluminescence with reading after disclosure with substrate of enzyme Western lighting plus ECL (Perkin-Elmer, Waltham, MA, USA). For p62 detection, donkey anti-rabbit secondary antibody coupled to IRdye 680 (LI-COR, Lincoln, NE, USA , 1:15000) was added for 1 hour at room temperature with stirring for reading on the LI-COR (ODYSSEY®FC , Lincoln , NE, USA) on the channel 700. Actin levels were measured by chemiluminescence using a mouse anti-actin (1:50,000, monoclonal Anti-β-Actin-Peroxidase antibody, Sigma-Aldrich®, St Louis, MO, USA). LC3II/actin and p62/actin ratios were calculated from respective protein determinations.

Statistical Analysis

Results of liver solutes were expressed as mean and standard deviation and similarly for enzymes after a log-transform to normalize their distribution and homogenize their variances. The impact of experimental conditions on their evolution during the 135 min perfusion was tested by *Zerbe's method for growth and response curves,* which allows comparing groups at each time point and over any time interval. For glycogen content and ratios, data were displayed as boxplots (median and interquartile range). Changes between T_0 and T_{135} were assessed by the *Wilcoxon signed rank test* while the *Kruskal-Wallis test* was used for between group comparisons. Calculations and graphs were done using SAS (version 9.4) and R (version 3.2.2) statistical packages. Significance was considered at the 5% critical level ($p < 0.05$).

Results

Perfusate marker liver solutes

Fig. 1A illustrates time-dependent changes in perfusate solutes in the four experimental groups. Perfusate glucose concentrations in fed group were systematically higher (p<0.0001) than in 18h, 24h and 24h+3MA fasting groups and likewise for lactate values. Glucose and lactate concentrations were also significantly lower (p<0.0001) in 18h-fasting group than in the two 24h-fasting groups. Potassium concentrations in fed group were significantly lower than in 18h-fasting (p<0.05) and 24h-fasting+3MA groups (p<0.001) after 90 min and 60 min of perfusion, respectively. They were also lower in 24h-fasting group than in 24h-fasting+3MA group after 75 min (p<0.01).

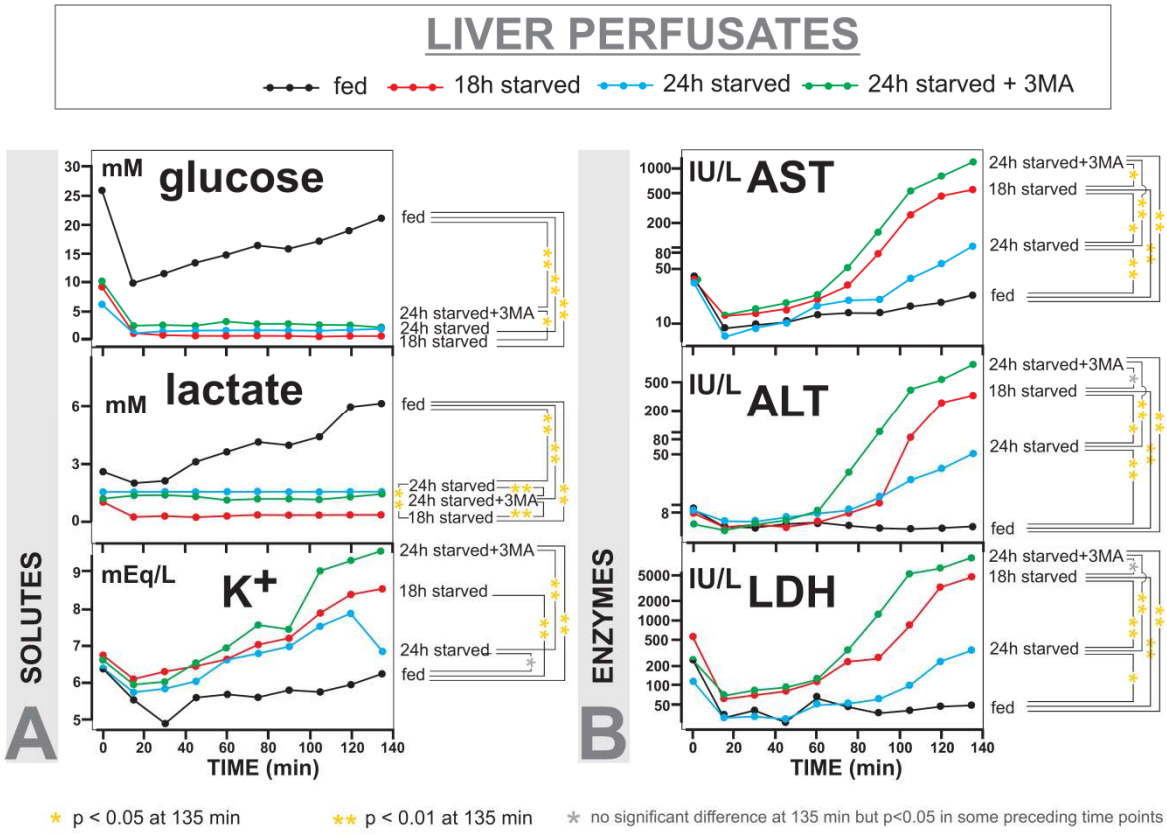

Fig. 1. Perfusate markers of *ex vivo* rat livers in fed, 18h-starved, 24h-starved and 24h-starved+3MA groups. Perfusate concentrations of solutes (**A**) and enzyme activity (**B**) over time are expressed in normal and logarithmic scaling, respectively with significant statistical differences between liver groups being given for values at the 135 min time point. Abbreviations: 3MA, 3-methyladenine; AST, aspartate transaminase; ALT, alanine transaminase; LDH, lactate dehydrogenase. Note that in contrast to all other ordinate scales which start from the zero, the ordinate scale of perfusate kalium starts at a 5 mEq/L value.

Perfusate marker liver enzymes

Liver enzyme releases in perfusate samples are illustrated in Fig. 1B. Values statistically significant are depicted for each group at 135 minutes. However, the kinetics of the considered enzyme release showed also significant differences from 60 to 120 minutes over the perfusion period. Basically, enzyme levels in 24h-fasted group were observed between those of fed and 18h-starved groups but highest enzyme activities were recorded in 24h-fasting+3MA group. AST values were significantly

lower in fed group than in the other three groups (p<0.001). AST in 24h-fasting group was significantly lower than in 24h-fasting+3MA (p<0.001) and 18h-fasting (p<0.05) groups. After 90 min of perfusion, AST curves were highest in 24h-fasting+3MA group and lowest in fed group; intermediate with values, however, higher in 18h- *vs* 24h-fasting groups (p=0.025). Similar findings were obtained for ALT. At the end of perfusion, ALT activities in 18h-fasting and 24h-fasting+3MA groups were not significantly different, these two groups having higher perfusate ALT levels than 24h-fasting group. LDH values differed between the four groups after 45 min of perfusion. They turned out to be systematically lower in fed group than in 18h-(p=0.014) and 24h-fasting+3MA (p=0.0001) groups but not 24h-fasting group. LDH values in 18h-fasting and 24h-fasting+3MA groups were similar and significantly higher than in 24h-fasting group.

Liver glycogen

At baseline, liver glycogen contents differed significantly between each group except between 24h-fasting and 24h-fasting+3MA (**Fig. 2** and **Fig. 3A**). During perfusion, it significantly decreased in all groups. At 135 min, glycogen was still in fed group higher than in 18h-fasted group (p<0.0001), the latter group exhibiting glycogen content higher than in the two 24h-fasted groups (p<0.0001). Glycogen content was lower in 24-fasting group than in 24h-fasting+3MA (p=0.014).

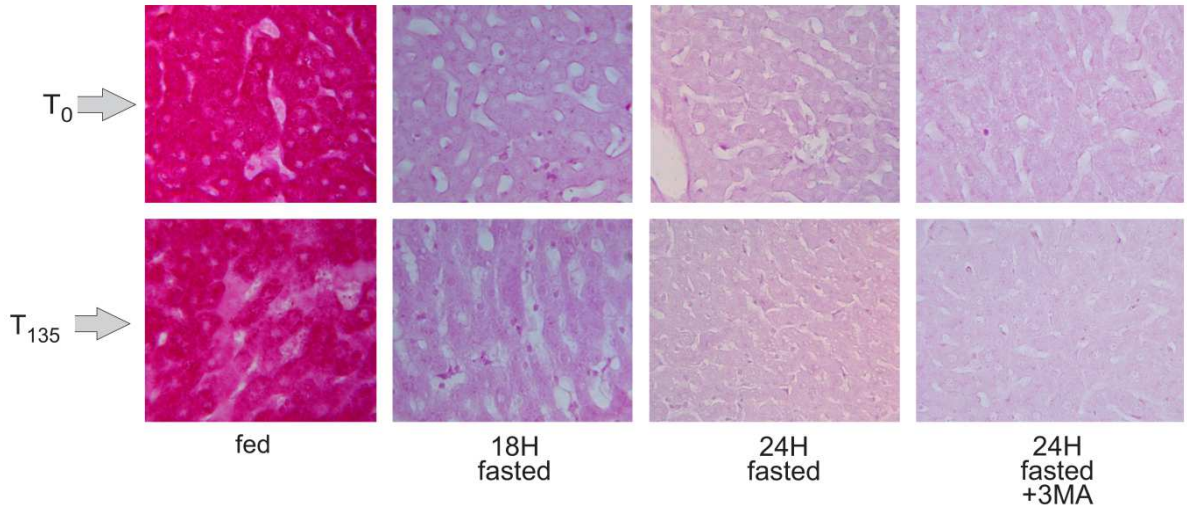

Fig. 2 - Photomicrographs of PAS-stained liver slices at 0 min (T_0) and 135 min(T_{135}) time-points in fed, 18-h starved, 24 h starved and 24h-starved + 3MA groups. The figure compares and illustrates for one animal in each nutritional group PAS staining at the start and end of liver perfusions. The abundance of glycogen is proportional to the red component of the PAS staining. As mentioned in the Materials and methods section, PAS stained slices were processed for determination of glycogen contents in hepatocytes at two time-points, i.e. 0 and 135 min, using the Image J software (National Institutes of Health, Bethesda, MD, USA). The electronically determined staining intensity values determined on the whole experimental groups are further accounted for by the boxplot representations appearing on Fig. 3 panel A.

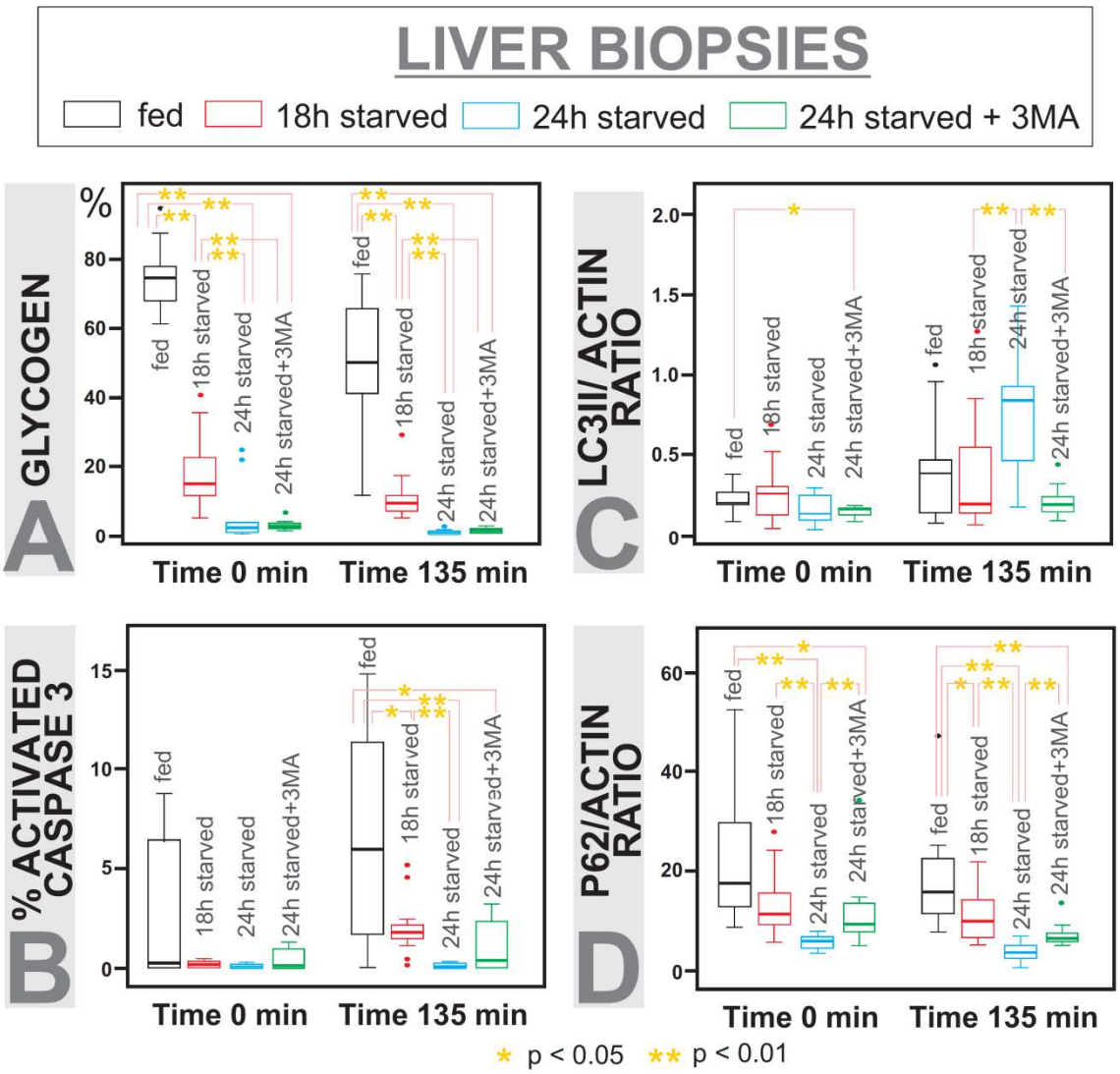

Fig. 3. Liver markers of *ex vivo* rat livers in fed, 18h-starved, 24h-starved and 24h-starved+3MA groups. Box plots account for glycogen content (**A**), apoptosis activated caspase-3 (**B**), autophagy specific LC3 II/actin (**C**) p62/actin (**D**) ratios. Significant statistical differences between liver groups are given for values at 0 min and at 135 min time points. Abbreviations: 3MA, 3-methyladenine

Liver apoptosis

Photomicrographs of activated caspase-3 liver immunohistochemistry at 0 min (T0) and 135 min (T135) time-points in fed, 18-h starved, 24 h starved and 24h-starved + 3MA groups are shown in **Fig. 4**. Apoptosis activity as measured by the percentage of activated caspase-3 was the same in all groups at baseline (**Fig. 3B**). At the end of perfusion, it differed between all groups except when comparing 24h-fasting+3MA with 18h- and 24h-fasting groups (**Fig. 3B**).

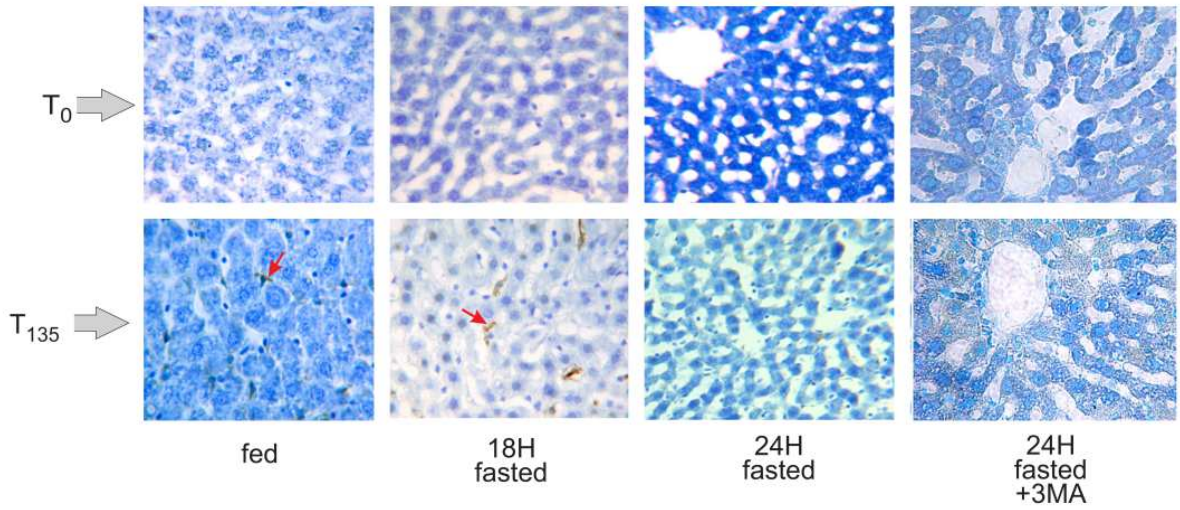

Fig. 4 - Photomicrographs of activated caspase-3 liver immunohistochemistry at 0 min (T_0) and 135 min(T_{135}) time-points in fed, 18-h starved, 24 h starved and 24h-starved + 3MA groups. The figure compares and illustrates for one animal in each nutritional group the immunolabelling at the start and end of liver perfusions. The red arrow appearing on 2 photomicrographs, namely those at 135 min for both fed and 18h-starved liver conditions, points to one of the immunolabelled cells seen on these liver photomicrographs. The immunolabelling is indicated by the visible brown coloration on photomicrographs (counterstaining being achieved by toluidine blue). As mentioned in the Materials and methods section, apoptosis counting was performed with the image J software using selection of cells immunolabelled for activated caspase-3, a determination of total and labelled cells by the image J cell counter and subsequent calculation of labelled to total liver cell ratios. These counting values determined on the whole experimental groups are accounted for by the boxplot representations appearing on Fig. 3 panel B.

Liver autophagy

LC3 II/actin ratio

The LC3II/actin ratio was similar in all groups at baseline but after 135 min of perfusion it was found significantly higher in 24h-fasting group than in 18h-fasting and 24h-fasting+3MA groups, respectively. During perfusion, LC3II/actin values significantly increased in 24h-fasting group but remained unchanged in other groups. The rise in autophagy was essentially lost under 3MA (**Fig. 3C**). **Fig. 5** visualizes western blotting bands of autophagy LC3II and actin in livers after 135 min *ex vivo* perfusion in fed, 18-h starved, 24 h starved and 24h-starved + 3MA groups.

p62/actin ratio

Fig. 5 also visualizes western blotting band of p62 (along with actin) in the various groups. As accounted for by boxplot representations appearing in **Fig 3D** panel, the p62/actin ratio differed significantly between groups at baseline, being higher in fed group than in 24h-fasting and 24h-fasting+3MA groups and lower in 24h-fasting than in 18h-fasting and 24h-fasting+3MA groups. During perfusion, it decreased in 18h-fasting and in 24h-fasting groups but not in fed and 24h-fasting+3MA groups (**Fig. 3D**). At 135 min, p62/actin ratio in fed group was still higher than in other groups. Interestingly, it was also higher in 18h-fasting group than in 24h-fasting and 24h-fasting+3MA groups.

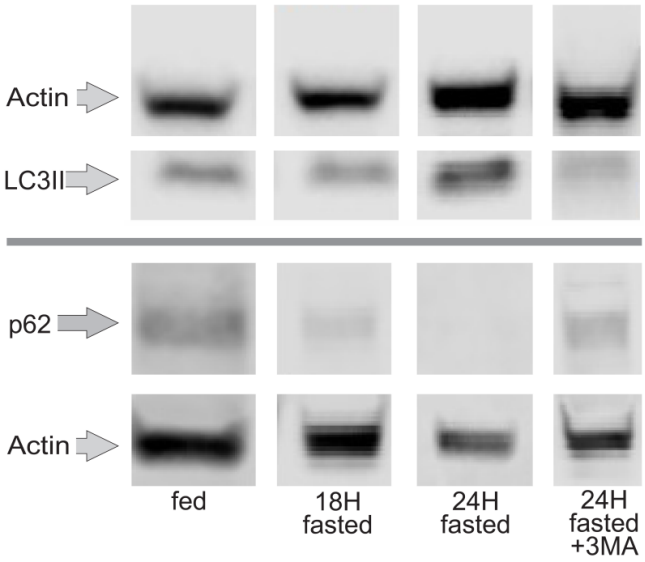

Fig.5 - Western blotting bands of autophagy LC3II and p62 proteins and actin in livers after 135 min *ex vivo* perfusion in fed, 18-h starved, 24 h starved and 24h-starved + 3MA groups. The figure compares and illustrates for one animal in each nutritional group that two separate runs were performed for assessing autophagy markers: one run for LC3II and a separate run for p62, each of these runs being also evaluated for actin content. The LC3II and p62, along with actin associated with each of these runs were quantified by LI-COR software on selected areas. Data generated by the LI-COR are highly reproducible and are not dependent on the operator and light exposure of blots. LI-COR data were used for boxplot representations appearing in Fig. 3 panels C and D.

Discussion

In perfused *ex vivo* livers, protective mechanisms were previously suggested to require energy availability being above a critical threshold [1]. In the present work, induction of autophagy was attested by a rise in LC3II/actin ratio and a drop in p62/actin ratio, which represent highly specific [1] and less specific markers of autophagy, respectively [10-12]. It was observed on transition from 18h to 24h-fasting and protected against fasting-driven exacerbation of liver vulnerability. In fasted groups, the link between protection against cytolysis and enhanced autophagy is stronger and more consistent than the link between protection and reduced apoptosis. After 135 min energy-free perfusion, cytolysis was significantly lower and autophagy higher in 24h-fasting group compared to 24h-fasting+3MA and 18h-fasting groups. Moreover, an inverse relationship between cytolysis and available energy sources (glycogen + autophagy) clearly emerges when comparing the four experimental groups. As illustrated by Fig. 6, the inverse link between autophagy and cytolysis is adequately highlighted when considering autophagy as taking part, along with glycogen stores, to cellular energy mobilization capacities.

Because *ex vivo* liver is disconnected from circulating energetic substrates and infused with energy-free perfusion, glycogen represents a major energetic source. This latter is by far lower in fasted than in fed livers (Fig. 3A). Enhanced autophagy, known to providing cells with energetic substrates [15], would compensate for limited glycogen stores and protect against reduced energy stores. The higher energy mobilization capacity, the lower is cytolysis (Fig. 6). Accordingly, inclusion of 3MA in perfusion reduced autophagic activity (Fig. 3 C and D); it led to increased cytolysis (Fig. 1B) and hence loss of benefit given by 24h- *vs* 18-fasting of rats, emphasizing that autophagy is well protective.

A key determinant in interpreting changes in levels of released metabolites, in particular lactate, is disconnection of *ex vivo* livers from circulation, opposing *ex vivo* and *in situ* livers. For *in situ* liver, lactate release in circulation is primarily fuelled from extra-hepatic anaerobic glycolysis to contribute

to Cori's cycle [16]. For perfused *ex vivo* livers, lactate release in perfusate, though virtually issued from anaerobic glycolysis by extra-hepatocyte cells (Kupffer, vascular, duct cells, etc.) primarily accounts for, like glucose, hepatocyte gluconeogenesis. Indeed, due to the absence of inclusion of glucose in perfusion and disconnection from circulation, the major glucose source from which lactate may derive is therefore hepatocyte gluconeogenesis, shading that, in return, lactate production depends on extra-hepatocyte glycolysis rates and may aliment hepatocyte gluconeogenesis. Though perhaps paradoxical, higher glucose production in fed *vs* fasted conditions is indicative of higher glycogen stores [17]. Accordingly, lactate release is higher in fed *vs* fasted livers (**Fig. 1A**). As regards to fasted livers, higher lactate levels at 24h- *vs* 18h-fasting might be explained by a higher background hepatocyte gluconeogenesis, perhaps as a result of a longer *in vivo* exposure to glucagon which interestingly, in contrast to the autophagy inhibitor insulin [18], promotes autophagy [19]. This higher lactate levels at 24h- *vs* 18h-fasting is not affected by inclusion of 3MA in perfusion; suggesting little or no compound effect on gluconeogenesis. Higher gluconeogenesis rates in the two 24h *vs* the one 18h-fasting groups might take place by consuming glycogen explaining why glycogen contents were significantly lowered in former *vs* latter groups. The significant drop however observed between hepatic glycogen contents of former groups (24h-fasting *vs* 24h-fasting+3MA) is only very moderate and might be accounted for by glycogen autophagy, a special form of autophagy referred to as glycophagy [20] and most likely to be eliminated under autophagy inhibition by 3MA.

Taken as a whole, present protective mechanisms are well accounted for by **Fig. 6**. Due to the present use of female animals, their potentiating by estrogen signalling cannot be ruled out. Since the pioneer work of de Duve, a growing-up attention has been dedicated to the role of autophagy in programmed cell death and optional survival through well designed experimental works [21-23]. In parallel and meanwhile, the clinical relevance of autophagy has also emerged in medical fields including surgery and oncology. Recently, the prognostic value of the autophagic marker LC3 was highlighted in two cohorts of patients undergoing liver resection as a surgical cure of hepatocellular carcinoma [24]. In this respect, liver regeneration after extended resections following neoadjuvant therapies represents a main issue where ischemic tolerance and remnant volume are of major interest. In the light of the present work, these experimental and medical developments might also stress the interest in promoting cellular pathways involved in energy mobilization to trigger protective and survival effects.

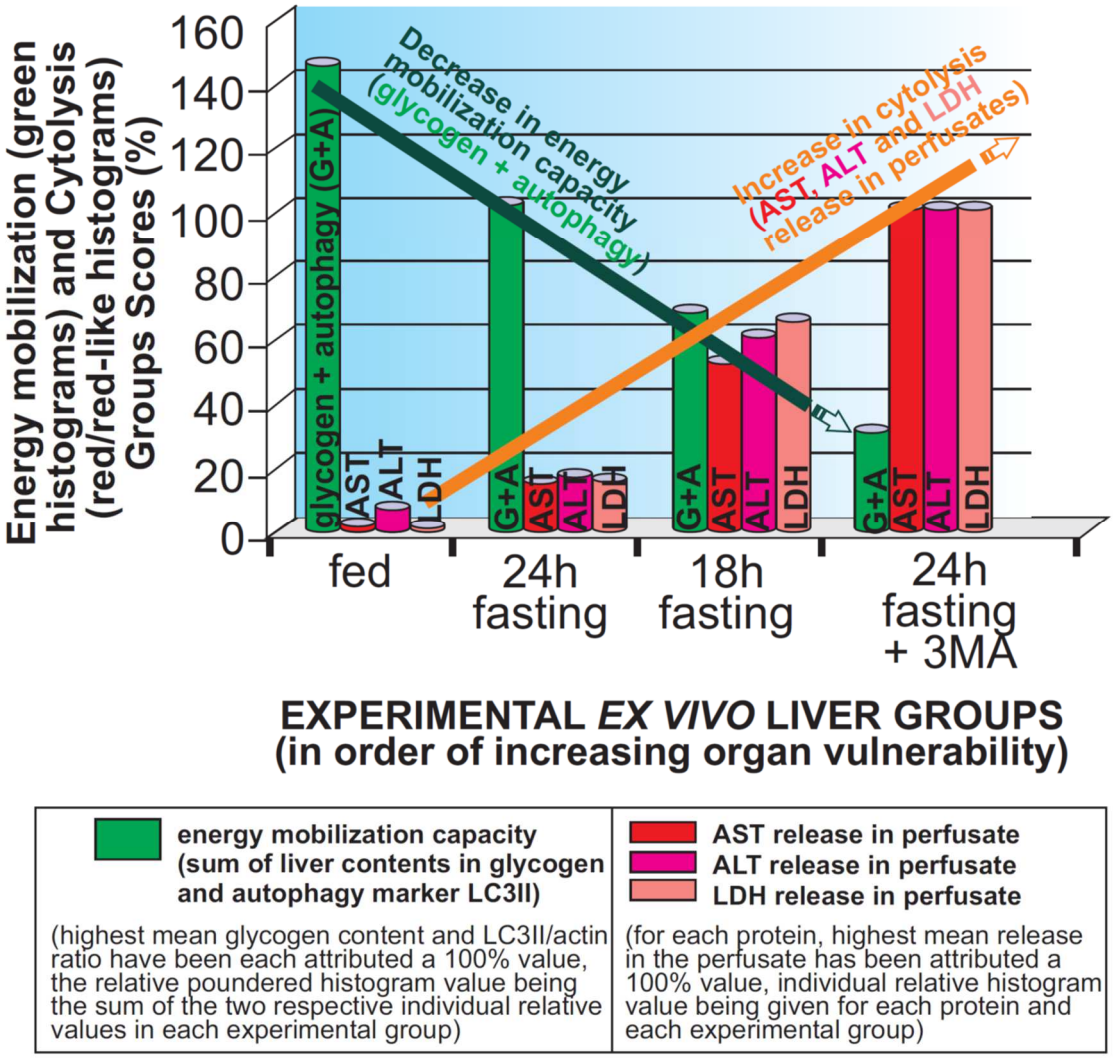

Fig. 6. Energy mobilization capacities *vs* cytolysis in *ex vivo* livers after exposure to a 135 min energy-free perfusion. Energy mobilization capacity in perfused *ex vivo* liver is essentially accounted for by the sum of glycogen stores and autophagic activity (assessed by LC3II/actin ratio) in liver biopsies (Fig. 3A and 3C, respectively). Cytolysis is accounted for by releases of AST, ALT, and LDH in perfusates (Fig. 1B). Relative mean levels of energy mobilization capacity and proteins released in perfusates are expressed as percentage values, the 100% mean value referring to the highest level throughout experimental groups. Accordingly, a 100% mean value has been ascribed to glycogen from fed livers, to autophagy marker LC3II/actin ratio from 24h-starved livers, and to AST, ALT and LDH releases from 24h-starved+3MA livers. For protein releases in perfusate, the three calculated percentages are individually represented (red and red-like histograms). For energy mobilization capacity (green histograms), calculated percentages of glycogen and LC3II/actin ratio have been summed (so percentage may exceed 100). The inverse relationship between energy mobilization capacity and cytolysis essentially accounts for protective roles of glycogen stores in fed conditions and of autophagic activity in starved conditions.

References

[1] Papegay B, Stadler M, Nuyens V, et al. Short fasting does not protect perfused ex vivo rat liver against ischemia-reperfusion. On the importance of a minimal cell energy charge. Nutrition 2017;35:21-27.

[2] Lemasters JJ, Nieminen AL, Qian T, et al. The mitochondrial permeability transition in cell death: a common mechanism in necrosis, apoptosis and autophagy. Biochim Biophys Acta 1998;1366:177-196.

[3] Liu Y, Levine B. Autosis and autophagic cell death: the dark side of autophagy. Cell Death Differ 2015;22:367-376.

[4] Kiraz Y, Adan A, Kartal Yandim M, et al. Major apoptotic mechanisms and genes involved in apoptosis. Tumour Biol 2016; 37: 8471-8486.

[5] Green DR. Apoptotic pathways: ten minutes to dead. Cell 2005;121:671-674.

[6] He C, Klionsky DJ. Regulation mechanisms and signaling pathways of autophagy. Annu Rev Genet 2009;43:67-93.

[7] Stipanuk MH. Macroautophagy and its role in nutrient homeostasis. Nutr Rev 2009; 67: 677-689.

[8] Stadler M, Nuyens V, Seidel L, et al. Effect of nutritional status on oxidative stress in an ex vivo perfused rat liver. Anesthesiology 2005;103:978-986.

[9] Hengartner MO. The biochemistry of apoptosis. Nature 2000;407:770-776.

[10] Barth S, Glick D, Macleod KF. Autophagy: assays and artifacts. J Pathol 2010;221:117-124.

[11] Klionsky DJ, Abdelmohsen K, Abe A, et al. Guidelines for the use and interpretation of assays for monitoring autophagy (3rd edition). Autophagy 2016;12:1-222.

[12] Mizushima N, Yoshimori T. How to interpret LC3 immunoblotting. Autophagy 2007;3:542-545.

[13] Seglen PO, Gordon PB. 3-methyladenine: specific inhibitor of autophagic/lysosomal protein degradation in isolated rat hepatocytes. Proc Natl Acad Sci USA 1982;79:1889–1892.

[14] Stadler M, Nuyens V, Boogaerts JG. Intralipid minimizes hepatocytes injury after anoxia-reoxygenation in an ex vivo rat liver model. Nutrition 2007;23:53-61.

[15] Singh R, Cuervo AM. Autophagy in the cellular energetic balance. Cell Metab 2011; 13: 495-504.

[16] Cori CF. The glucose-lactic acid cycle and gluconeogenesis. Curr Top Cell Regul 1981;18:377-387.

[17] Hems DA, Whitton PD. Control of hepatic glycogenolysis. Physiol Rev 1980;60:1-50.

[18] Paula-Gomes S, Gonçalves DA, Baviera AM, et al. Insulin suppresses atrophy- and autophagy-related genes in heart tissue and cardiomyocytes through AKT/FOXO signaling. Horm Metab Res 2013;45:849-855.

[19] Schworer CM, Mortimore GE. Glucagon-induced autophagy and proteolysis in rat liver: mediation by selective deprivation of intracellular amino acids. Proc Natl Acad Sci USA 1979; 76: 3169-3173.

[20] Jiang S, Wells CD, Roach PJ. Starch-binding domain-containing protein 1 (Stbd1) and glycogen metabolism: Identification of the Atg8 family interacting motif (AIM) in Stbd1 required for interaction with GABARAPL1. Biochem Biophys Res Commun 2011; 413:4 20-25.

[21] De Duve C, Wattiaux R. Functions of lysosomes. Annu Rev Physiol 1966;28:435-492.

[22] Komatsu M, Waguri S, Ueno T, Iwata J, Murata S, Tanida I, Ezaki J, Mizushima N, Ohsumi Y, Uchiyama Y, Kominami E, Tanaka K, Chiba T. Impairment of starvation-induced and constitutive autophagy in Atg7-deficient mice. J Cell Biol 2005;169:425-434.

[23] Mortimore GE, Pösö AR. Intracellular protein catabolism and its control during nutrient deprivation and supply. Annu Rev Nutr 1987;7:539-564.

[24] Lin CW, Lin CC, Lee PH, et al. The autophagy marker LC3 strongly predicts immediate mortality after surgical resection for hepatocellular carcinoma. Oncotarget 2017;8:91902-91913.

GRAPHICAL ABSTRACT